Research Article

THERMODYNAMIC ANALYSIS OF A NOVEL COMBINED SUPERCRITICAL CO2 AND ORGANIC RANKINE CYCLE

Authors: Ahmet Elbir Mehmet Erhan Şahin Arif Emre Özgür Hilmi Cenk Bayrakçı

To cite to this article: Elbir, A. , Şahin, M. E. , Özgür, A. E. & Bayrakçı, H. C. (2023). THERMODYNAMIC ANALYSIS OF A NOVEL COMBINED SUPERCRITICAL CO2 AND ORGANIC RANKINE CYCLE . International Journal of Engineering and Innovative Research ,5(1), p33-47. DOI: 10.47933/ijeir.1187448

DOI: 10.47933/ijeir.1187448

To link to this artice: https://dergipark.org.tr/tr/pub/ijeir/archive

International Journal of Engineering and Innovative Research

http://dergipark.gov.tr/ijeir

THERMODYNAMIC ANALYSIS OF A NOVEL COMBINED SUPERCRITICAL CO_2 AND ORGANIC RANKINE CYCLE

Ahmet Elbir[1*], Mehmet Erhan Şahin[2], Arif Emre Özgür[3], Hilmi Cenk Bayrakçı[3]

[1]Suleyman Demirel University, YEKARUM, Isparta, Turkey.
[2] Isparta Applied Science University, Technical Vocational High School, Isparta, Turkey.
[3]Isparta Applied Science University, Technology Faculty, Isparta, Turkey.

[*]Corresponding Author: ahmetelbir@sdu.edu.tr
(**Received:** 11.10.2022; **Accepted:** 25.11.2022)

DOI: 10.47933/ijeir.1187448

ABSTRACT: Sustainable and innovative technologies offer us the inevitable opportunity to use the last drop of energy. In this study, gradual compression and gradual expansion were carried out with intermediate heat exchangers in single and double stage S-CO_2 brayton cycles operating at the same operating temperature ranges. The ORC (Organic Rankine Cycle) is integrated from the system's waste heat source. The performance characteristics of the S-CO_2 power systems and the combined ORC system, as well as the energy and energy analysis results of the system components for each component, are presented in tables. The performance of the gradual compression and gradual expansion systems, the operating conditions of the stepless system operating under the same operating conditions, were examined. It has been reported that there is an increase in electricity generation of 136% and an increase in thermal efficiency of 22% when switching from single-stage to double-stage. The addition of the ORC system to the single-stage and double-stage systems increased the thermal efficiency by 10.2% and the net work by 39.75KW. When switching from single stage to double stage, exergy destruction increased by 86% and energy efficiency decreased by 1%. The addition of the ORC system to the single-stage and double-stage systems increased the energy efficiency by 15% and the exergy destruction by 44.27KW. As a result, nature-friendly CO_2 shows us that it is an alternative, innovative, and sustainable source in low temperature applications.

Keywords: Brayton cycle, S-CO_2, ORC, Enegy analysis, Exergy analysis.

1. INTRODUCTION

In recent days, we have seen that global problems increase the demand for energy needs with the effects of the pandemic. The common views of international agencies say that the demand for electricity will increase further, the need for primary fossil resources will increase to meet this demand, and the result will be met mostly by coal. The use of coal pollutes our atmosphere with high levels of CO_2, SO_2, NOx, and CO_2. We know that the main elements of the environmental problems faced by humanity are the improvement of energy efficiency and the reduction of carbon emissions. In this context, it has led us to use traditional fossil fuel energy sources in a more sustainable and rational way, not in an alarming way. As a result, the environmental friendliness of energy and the increase in its efficiency have led us to combined power systems. When choosing environmentally friendly energy sources, we should choose renewable energy sources such as solar, wind, biomass and geothermal. In power generation

systems, S-CO_2 (Supercritical carbon dioxide) is the most promising and environmentally friendly system. When we look at the latest studies, ensuring that unused waste heat is converted into energy without being thrown into the environment will reduce the negative environmental effects. We see that it provides additional benefits, especially in converting waste heat sources to power generation systems with ORC systems. If we look at how environmentally friendly CO_2 systems are used in electricity generation in the literature; Wang, et al., suggested CO_2 power cycles in their work. If the source temperature is high, CO_2 power systems have better efficient than the Rankine cycle having ultra-supercritical operating conditions. CO_2 power cycles are also an innovative approach to power production, notedly for low-grade heat sources. [1]. Mishra and Kumar, studied the thermodynamic performance of the Brayton Cycle. They claim that the Brayton cycle powered by R123 outperforms R245fa and R134a in terms of thermodynamic performance. They studied how various performance parameters, such as pressure ratio, maximum temperature in the cycle, and compressor inlet temperature, affect the Brayton cycle [2]. Bellos, and Tzivanidis, investigated a transcritical refrigeration cycle connected to a Brayton cycle with a CO_2 recompression fed by a biomass boiler [3]. Deng et al., compared the application of thermal source temperatures in the Brayton cycle (recompression, intercooling, and reheating). They said that with increasing temperature of the heat source, the efficiency of the recompression model gradually increased [4]. Zhang et al., performed the related system design and thermodynamic analysis to analyze the energetic and exergetic performance of the supercritical power cycle. They investigated the parametric values of turbine inlet temperatures and operating pressures. They said that high pressure increases the turbine's temperature and increases cycle efficiency while reducing output work. In this case, for the effect of low pressure turbine inlet temperature, it is said that the cycle efficiency and output work increase with increasing temperature. They stated that the waste heat recovery efficiency in the system they studied increased to 74.83% [5]. Hoang et al., In their evaluation of S-CO_2 Brayton Energy Conversion Systems, they investigated the effects of changing thermodynamic assumptions and investigated the effect of non-ideal fluid behavior on heat exchanger performance [6]. Wang et al., evaluated the effects of key thermodynamic parameters on the performance of combined S-CO_2, T-CO_2 cycles. They showed that the thermal efficiency of the simple S-CO_2, T-CO_2 cycle at S-CO_2 turbine pressure ratio and compressor inlet temperature increased [7]. Yari and Sirousazar, This study investigated the performance of the pre-cooler recompression S-CO_2 Brayton cycle used in a transcritical carbon dioxide (T-CO_2) cycle to improve the performance of the cycle. They also made a comparison between S-CO_2 and a simple S-CO_2 cycle. They said that both the energetic and exergetic efficiencies of the new S-CO_2 cycle are about 5.5 percent to 26 percent higher than the simple S-CO_2 cycle [8]. Al-Sulaiman and Atıf made a comparison five different supercritical carbon dioxide Brayton cycles operated with the energy obtained from a solar tower. Split expansion Brayton cycle, precompression Brayton cycle, recompression Brayton cycle, regenerative Brayton cycle, and Brayton cycle analyses were carried out. They showed that recompression Brayton cycle have the highest thermal efficiency. The regenerative Brayton cycle, although leaner in configuration, performs comparable to the recompression Brayton cycle. [9]. Yu et al., They said that the internal combustion engine (ICE) with waste heat recovery and S-CO_2 cycle is considered a promising technology [10]. Casanova et al., Transcritical carbon dioxide cycles and the Rankine cycle have arised as alternatives for power generation in low-temperature applications. The low heat removal temperatures required for CO_2 condensation are prohibitive for many locations. They studied the S-CO_2 Brayton cycle [11]. Zhoua et al., presented the second law analysis of a single-reheated S-CO_2 Brayton cycle for coal-fired power plant. They emphasized that the optimum parameters of the turbines provide a higher expansion rate for the low pressure turbine (LPT) than for the high pressure turbine (HPT). They showed that the overall energy efficiency of a reheated 1000MW S-CO_2 coal-fired power

plant is higher than that of a conventional ultra-high critical steam plant [12]. Chowdhury et al., The S-CO_2 Brayton cycle S-CO_2, triple cycle (TLC), and ORC examined the performance of the cycles under constant heat input conditions. They showed that a higher thermal efficiency (26.5%) can be achieved in the case of the ORC cycle with n-pentane as the working fluid, compared with S-CO_2 and TLC with its thermal efficiency [13]. Wang et al., stated that the intercooling loop layout and sub-cooling loop layout usually provide the best performances, followed by the recompression loop layout and precompression loop layout, while the simple recovery loop layout has the worst performances. They said that the advantages of partial refrigeration loop layout and intercooling loop layout are more pronounced in the case of high compressor inlet temperatures compared to other loop layouts [14]. Wei et al., analyzed the S-CO_2 Brayton cycle and the ORC combined system [15]. Ma and Liu., it is said that it will be a creative power system by integrating the S-CO_2 Brayton cycle with the transcritical ORC. They said that the ORC turbine and the CO_2 turbine have a priority of improvement over the compressor and pump. They showed that the ORC increases the maximum system energy efficiency by changing the turbine inlet pressure [16]. Wang et al., in their study, they presented comparative research on the supercritical carbon dioxide power cycle for waste heat recovery of gas turbines. From cycles, energy and exergy analyses were optimized according to single and multi-objective optimization results from the perspective of system efficiency, configuration complexity, and economic cost. They emphasized the importance of increasing the thermal efficiency of the gas turbine waste heat recovery system. They emphasized the use of a double-heated cascade cycle to ensure high system efficiency [17]. Purjam, et al., projecting new and efficient heat machines and increasing their efficiency is one of the interests of researchers in the field of thermodynamics. In this context, they designed a cycle with the favorable features of familiar cycles, such as less emission and higher power-to-weight ratio and efficiency. The supercritical carbon dioxide cycle (SCDC) is assumed that one of the most promising cycle. The main aim of this research is to design a high efficiency SCDC with an efficiency of 45% to 47%. They said that this article includes the entire designed loop, designing and discussing efficiency improvement methods, comparing, designing, and discussing SCDC with other power loops. The sensitivity of loop efficiency to some important parameters was also examined [18]. Padilla et al., In this paper, thermodynamic analyses are performed separately for each component of a supercritical CO_2 recompression Brayton cycle. As a result, they showed that the energy efficiency reached its maximum value at 600 °C and that the first law efficiency increased with the temperature of the cycle. [19]. Besarati at al. In this study, S-CO_2 Brayton cycle, recompression S-CO_2 Brayton cycle and partial cooling S-CO_2 Brayton cycles are compared with the studies in the literature. They have added an ORC to each configuration to take advantage of the waste heat source. Different working fluids were used for these integrated cycles and the working conditions were analyzed. showed that the combined recompression-ORC cycle provides higher thermodynamic efficiency than other systems. [20]. Akbari at al., presented an exergoeconomic analysis analyzed for a new combined S-CO_2 recompression Brayton and organic Rankine cycle (SCRB/ORC). In this project, waste heat from the SCRBC is used by an ORC to generate power. Thermodynamic and exergoeconomic analyzes are also studied to make comparisons for eight different ORC working fluids with models were developed. The results showed that the best energy efficiency and lowest product unit cost for SCRB/ORC were obtained when isobutane and RC318 ORC working fluid were considered, respectively [21]. Khan and Mishra, This study performed a performance analysis of a combined pre-compression S-CO_2 cycle and ORC powered by a solar tower for waste heat recovery. The results showed that the net power output and thermal efficiency of the pre-compression loop were improved by 4.51% and 4.52%, respectively, using ORC. They said that the combined cycle's highest thermal, energy efficiency and power output increased with 1000 W/m^2 of solar radiation using R227ea, and the solar radiation with the highest values was

51.83 – 74.06%, and 278.5 kW. They emphasized that the efficiency of the heat exchanger increases the waste heat recovery rate. They found the best value as 0.5673 at 0.95 efficacy according to R227ea [22]. Chacartegui at al., In this study, low-temperature ORC was investigated as a sub-cycle in medium and large-scale combined cycle power plants. As organic fluids, cyclohexane, R245, isobutene, R113, toluene, and isopentane toluene were used. Of these, competitive results were obtained for the cyclohexane ORC combined cycles. [23].

When S-CO_2 systems are examined in the literature, it is seen that they are either single-stage or double-stage. In our study, the thermodynamic analysis of the single-stage, single-expansion S-CO_2/ORC system, operating at the same lower and upper temperatures as the single-stage, double-expansion S-CO_2/ORC system, was investigated. In the study, environmentally-friendly R600a refrigerant was used in the ORC system. Recent system improvements for CO_2 have been made in supercritical Brayton cycles with intermediate heat exchangers, gradual compression, and gradual expansion. In the waste heat sources of the system, the gradual expansion of the ORC cycles is provided by the intermediate heat exchangers. Performance characteristics of S-CO_2 power systems and combined ORC systems are aimed at energy and exergy analysis of system components.

2. METHODS

2.1. System Description

Figure 1 gives a schematic of a single-stage S-CO_2 cycle for a closed-cycle supercritical CO_2 using CO_2 as the working fluid.

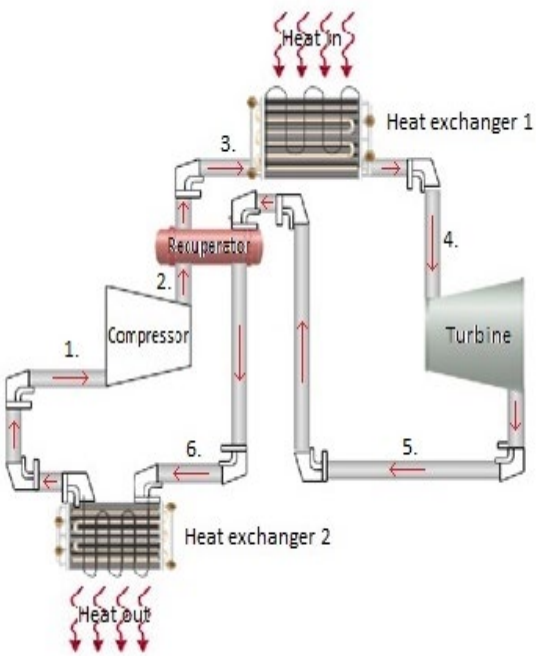

Figure 1. Single-stage S-CO_2 cycle.

The process location in the design is as follows:
1. 1→2: Adiabatic compressor increases fluid pressure and converts it to supercritical fluid,
2. 2→3: adiabatic heat transfer with counterflow recuperator.
3. 3→4: The working fluid receives heat from the heat source,

4. 4→5: expanding the adiabatic turbine to generate work
5. 5→6: adiabatic heat removal with counterflow recuperator.
6. 6→1: return to State I by isobaric transfer of the heat of the fluid to an ORC system

Combining a S-CO_2 closed loop cascade compression and cascade expansion system using CO_2 as the working fluid with the ORC system Figure 2 gives a schematic of the cycle.

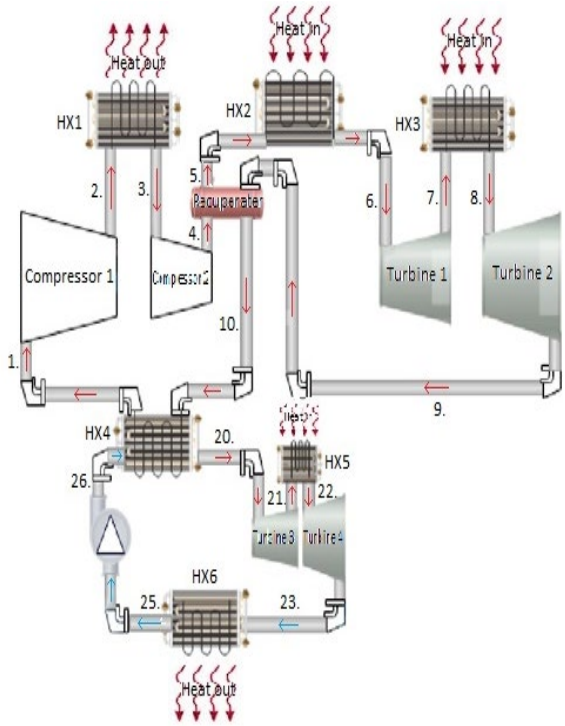

Figure 2. Double-stage expansion and double-stage compression combined with ORC in the S-CO_2 cycle.

The process location in the design is as follows:

1. 1→2: Adiabatic compressor-I increases the fluid pressure and converts it to supercritical fluid,
2. 2→3: lowering the isobaric temperature of the supercritical fluid in the heat exchanger,
3. 3→4: again increasing the fluid pressure of the Adiabatic compressor-II,
4. 4→5: adiabatic heat transfer with counter flow recuperator.
5. 5→6: The working fluid receives heat from the heat source,
6. 6→7: expanding the adiabatic turbine-I to generate work
7. 7→8: Reheating the working fluid up to the turbine-I inlet temperature,
8. 8→9: expanding the adiabatic turbine-II to generate work
9. 9→10: adiabatic heat removal with counter flow recuperator.
10. 10→1: return to State I by isobaric transfer of heat of the fluid to an ORC system.
11. 26→20: heat transfer from adiabatic and mixed flow heat exchanger to R600a ORC system
12. 20→21: expanding the adiabatic turbine-III to generate work
13. 21→22: Reheating the working fluid to turbine-III inlet temperature,
14. 22→23: Expanding the adiabatic turbine to generate IV work
15. 23→25: heat removal by heat exchanger as isobar.
16. 25→26: increasing the pressure of the saturated liquid with the adiabatic pump.

Thermodynamic equations

The following assumptions were taken into account while making the thermodynamic analysis of the system:

• Pure substance is used in the system.

• The compression in the compressor is adiabatic.
• Pressure drops in system components and on the pipeline and the heat transfer process are also neglected.
• All heat exchangers are counter flow.
• System performance is assumed to be constant and regular.
• Gravitational potential energy and kinetic energy are not taken into account.
• It has been calculated by taking the pressure ratio in the compressors and turbines, which are used in stages, as 1.8 as a constant.
• Isentropic efficiency of the compressors and pumps in the systems ηiz =0.85
• Isentropic efficiency for turbines in systems ηiz =0.90
• Ambient temperature is taken as 20 ºC.
• There was 40% more heat transfer from the source and 40% less heat transfer from all heat exchangers except the recuperator and heat exchanger 4.
• Calculations were made by taking the heat source and instantaneous surface temperature differences in the heat source heat exchangers, 10 K in the brayton cycle, and 2 K in the ORC.

2.2. Energy and exergy analyzes

For steady state in thermodynamic analysis, the basic mass balance equation can be given as follows;

$$\sum \dot{m}_{in} = \sum \dot{m}_{ex} \tag{1}$$

where $\dot{m}$ is the mass flow rate, the in and ex indices represent the inlet and outlet states, respectively. The energy balance is given as:

$$\dot{Q}_{in} + \dot{W}_{in} + \sum_{in} \dot{m}\left(h + \frac{V^2}{2} + gz\right) = \dot{Q}_{ex} + \dot{W}_{ex} + \sum_{ex} \dot{m}\left(h + \frac{V^2}{2} + gz\right) \tag{2}$$

Here, $\dot{Q}$ is the heat transfer rate, , $\dot{W}$ is the power, h is the specific enthalpy, v is the velocity, z is the height, and g is the gravitational acceleration. The entropy balance equation for steady-state conditions is written as:

$$\sum_{in} \dot{m}_{in} s_{in} + \sum_k \frac{\dot{Q}}{T_k} + \dot{S}_{gen} = \sum_{ex} \dot{m}_{ex} s_{ex} \tag{3}$$

where s is the specific entropy and $\dot{S}_{gen}$ is the entropy generation rate. The exergy balance equation can be written as:

$$\sum \dot{m}_{in}\, ex_{in} + \sum \dot{E}\, x_{Q,in} + \sum \dot{E} x_{W,in} = \sum \dot{m}_{ex} ex_{ex} + \sum \dot{E} x_{Q,ex} + \sum \dot{E} x_{W,ex} + \dot{E} x_D \tag{4}$$

The specific flow exergy can be written as:

$$ex = x_{ph} + ex_{ch} + ex_{pt} + ex_{kn} \tag{5}$$

The kinetic and potential parts of the exergy are assumed to be negligible. Also, the chemical exergy is assumed to be negligible. The physical or flow exergy (ex_{ph}) is defined as:

$$ex_{ph} = (h - h_o) - T_o(s - s_o) \tag{6}$$

where h and s represent specific enthalpy and entropy, respectively, in the real case. h_o and s_o are enthalpy and entropy at reference medium states, respectively.

The instantaneous temperature T(K) value for the surfaces was calculated as follows:

$$T = \frac{h_2 - h_1}{s_2 - s_1} \tag{7}$$

Exergy destruction is equal to specific exergy times mass;

$$\dot{E}x_D = ex * m \tag{8}$$

or

$$\dot{E}x_D = T_0 \dot{S}_{gen} \tag{9}$$

$\dot{E}x_W$, are work-related exergy ratios and are given as:

$$\dot{E}x_W = \dot{W} \tag{10}$$

$\dot{E}x_Q$, are the exergy rates related to heat transfer and are given as below.

$$\dot{E}x_Q = \left(1 - \frac{T_o}{T}\right)\dot{Q} \tag{11}$$

What work comes out of the system;

$$\dot{W}net_{out} = \dot{Q}_{in} - \dot{Q}_{out} \tag{12}$$

efficiency for the Brayton system;

$$\eta th, = \frac{\dot{W}net_{out}}{\dot{Q}_{in}} \tag{13}$$

The exergy efficiency (ψ) can be defined as follows;

$$\psi = \frac{\sum useful\ output\ exergy}{\sum input\ exergy} = 1 - \frac{\sum exergy\ loss}{\sum input\ exergy} \tag{14}$$

The mass balance, energy balance, entropy balance, exergy balance and exergy efficiency equations for each component are presented in Table 1.

Table 1. Mass balance, energy balance, entropy balance, exergy balance and exergy efficiency equations

Component	Mass balance	Energy balance	Entropy balance	Exergy balance	Exergy efficiency
CO_2-Comp1 (1-2)	$\dot{m}_1 = \dot{m}_2 = \dot{m}_{CO2}$	$\dot{W}_{Comp1.} = \dot{m}_{CO2}(h_2 - h_1)$	$\dot{S}_{gen,Comp1.} = \dot{m}_{CO2}(s_2 - s_1)$	$\dot{E}x_{D,Comp1} = \dot{m}_{CO2}(ex_1 - ex_2) + \dot{W}_{Comp1}$	$\psi_{copm1} = \frac{\dot{m}_{CO2}(ex_2 - ex_1)}{\dot{W}_{Comp1}}$
	$\dot{m}_2 = \dot{m}_3 = \dot{m}_{CO2}$	$\dot{Q}_{HXI}^{out} = \dot{m}_{CO2}(h_2 - h_3)$			

CO_2-heat exchanger I (2-3)		$\dot{Q}_{HX1}^{in} = \dot{m}_{CO2}(h_2 - h_3)/1{,}4$	$\dot{S}_{gen.,HX1} = \dot{m}_{CO2}(s_2 - s_3) + \left(\frac{\dot{Q}_{CO2}^{in}}{T_{HX1} - 10}\right)$	$\dot{E}x_{D,HX1} = \dot{m}_{CO2}(ex_2 - ex_3) - \dot{Q}_{CO2}^{in}\left(1 - \frac{T_0}{T_{HX1} - 10}\right)$	$\psi_{cond.} = \frac{\dot{Q}_{CO2}^{in}\left(1 - \frac{T_0}{T_{HX1} * 1{,}03}\right)}{\dot{m}_{CO2}(ex_2 - ex_3)}$
CO_2-Comp2 (3-4)	$\dot{m}_3 = \dot{m}_4 = \dot{m}_{CO2}$	$\dot{W}_{\mathbf{Comp2}} = \dot{m}_{CO2}(h_4 - h_3)$	$\dot{S}_{gen,Comp2.} = \dot{m}_{CO2}(s_4 - s_3)$	$\dot{E}x_{D,\mathbf{Comp2}} = \dot{m}_{CO2}(ex_3 - ex_4) + \dot{W}_{Comp2}$	$\psi_{comp2} = \frac{\dot{m}_{CO2}(ex_4 - ex_3)}{\dot{W}_{Comp2}}$
CO_2-Recuperator (4-5)	$\dot{m}_4 = \dot{m}_5 = \dot{m}_9 = \dot{m}_{10} = \dot{m}_{CO2}$	$\dot{m}_{CO2}(h_9 - h_{10}) = \dot{m}_{CO2}(h_5 - h_4)$	$\dot{S}_{gen,Rekü.} = \dot{m}_{CO2}(s_{10} - s_9) + \dot{m}_{CO2}(s_5 - s_4)$	$\dot{E}x_{D,Rekü.} = \dot{m}_{ORC}(ex_4 - ex_5) + \dot{m}_{ORC}(ex_9 - ex_{10})$	$\psi_{Rekü.} = \frac{\dot{m}_{CO2}(ex_5 - ex_4)}{\dot{m}_{CO2}(ex_9 - ex_{10})}$
CO_2-heat exchanger II (5-6)	$\dot{m}_5 = \dot{m}_6 = \dot{m}_{CO2}$	$\dot{Q}_{HX2}^{in} = \dot{m}_{CO2}(h_6 - h_5) * 1{,}4$ $\dot{Q}_{HX2}^{out} = \dot{m}_{CO2}(h_6 - h_5)$	$\dot{S}_{gen.,HX2} = \dot{m}_{CO2}(s_6 - s_5) + \left(\frac{\dot{Q}_{CO2}^{in}}{T_{HX2} + 10}\right)$	$\dot{E}x_{D,HX2} = \dot{m}_{CO2}(ex_5 - ex_6) + \dot{Q}_{CO2}^{in}\left(1 - \frac{T_0}{T_{HX2} + 10}\right)$	$\psi_{comp.} = \frac{\dot{m}_{CO2}(ex_5 - ex_6)}{\dot{Q}_{CO2}^{in}\left(1 - \frac{T_0}{T_{HX2} + 10}\right)}$
CO_2-Turbine I (6-7)	$\dot{m}_6 = \dot{m}_7 = \dot{m}_{CO2}$	$\dot{W}_{turb1.} = \dot{m}_{CO2}(h_6 - h_7)$	$\dot{S}_{gen,turb1.} = \dot{m}_{CO2}(s_7 - s_6)$	$\dot{E}x_{D,turb1.} = \dot{m}_{CO2}(ex_6 - ex_7) - \dot{W}_{turb1.}$	$\psi_{turb1.} = \frac{\dot{W}_{turb1.}}{\dot{m}_{CO2}(ex_6 - ex_7)}$
CO_2-heat exchanger III (7-8)	$\dot{m}_7 = \dot{m}_8 = \dot{m}_{CO2}$	$\dot{Q}_{HX3}^{in} = \dot{m}_{CO2}(h_7 - h_8) * 1{,}4$ $\dot{Q}_{HX3}^{out} = \dot{m}_{CO2}(h_7 - h_8)$	$\dot{S}_{gen.,HX3} = \dot{m}_{CO2}(s_8 - s_7) + \left(\frac{\dot{Q}_{CO2}^{in}}{T_{HX3} + 10}\right)$	$\dot{E}x_{D,HX3} = \dot{m}_{CO2}(ex_7 - ex_8) + \dot{Q}_{CO2}^{in}\left(1 - \frac{T_0}{T_{HX2} + 10}\right)$	$\psi_{HX3} = \frac{\dot{m}_{CO2}(ex_8 - ex_7)}{\dot{Q}_{CO2}^{in}\left(1 - \frac{T_0}{T_{HX3} + 10}\right)}$
CO_2-Turbine II (8-9)	$\dot{m}_8 = \dot{m}_9 = \dot{m}_{CO2}$	$\dot{W}_{turb2.} = \dot{m}_{CO2}(h_8 - h_9)$	$\dot{S}_{gen,turb2.} = \dot{m}_{CO2}(s_9 - s_8)$	$\dot{E}x_{D,turb2.} = \dot{m}_{CO2}(ex_8 - ex_9) - \dot{W}_{turb2.}$	$\psi_{turb2.} = \frac{\dot{W}_{turb2.}}{\dot{m}_{CO2}(ex_8 - ex_9)}$
CO_2-R600a heat exchanger IV (10-1) (20-26)	$\dot{m}_{10} = \dot{m}_1 = \dot{m}_{CO2}$; $\dot{m}_{26} = \dot{m}_{20} = \dot{m}_{R600a}$	$\dot{Q}_{R600a}^{in} = \dot{m}_{R600a}(h_{20} - h_{26}) * 1{,}4$ $\dot{Q}_{HX4}^{out} = \dot{m}_{CO2}(h_{10} - h_1)$	$\dot{S}_{gen.,HX4} = \dot{m}_{CO2}(s_{11} - s_{10}) - \dot{m}_{R600a}(s_{26} - s_{20})$	$\dot{E}x_{D,HX4} = \dot{m}_{CO2}(ex_{10} - ex_{11}) - \dot{m}_{R600a}(ex_{20} - ex_{26})$	$\psi_{HX4} = \frac{\dot{m}_{R600a}(ex_{20} - ex_{26})}{\dot{m}_{CO2}(ex_{10} - ex_{11})}$
R600a-Turbine III (20-21)	$\dot{m}_{20} = \dot{m}_{21} = \dot{m}_{R600a}$	$\dot{W}_{turb3.} = \dot{m}_{R600a}(h_{20} - h_{21})$	$\dot{S}_{gen,turb3.} = \dot{m}_{CO2}(s_{20} - s_{21})$	$\dot{E}x_{D,turb3.} = \dot{m}_{CO2}(ex_{20} - ex_{21}) - \dot{W}_{turb3.}$	$\psi_{turb2.} = \frac{\dot{W}_{turb3.}}{\dot{m}_{CO2}(ex_{20} - ex_{21})}$
R600a-heat exchanger V (21-22)	$\dot{m}_{21} = \dot{m}_{22} = \dot{m}_{R600a}$	$\dot{Q}_{HX5}^{out} = \dot{m}_{R600a}(h_{22} - h_{21})$ $\dot{Q}_{HX5}^{in} = \dot{m}_{R600a}(h_{22} - h_{21}) * 1{,}4$	$\dot{S}_{gen.,HX5} = \dot{m}_{R600a}(s_{22} - s_{21}) + \left(\frac{\dot{Q}_{CO2}^{in}}{T_{HX5} + 2}\right)$	$\dot{E}x_{D,HX5} = \dot{m}_{R600a}(ex_{21} - ex_{22}) + \dot{Q}_{CO2}^{in}\left(1 - \frac{T_0}{T_{HX5} + 2}\right)$	$\psi_{HX5} = \frac{\dot{m}_{R600a}(ex_{22} - ex_{21})}{\dot{Q}_{CO2}^{in}\left(1 - \frac{T_0}{T_{HX5} + 2}\right)}$

R600a-Turbine IV (22-23)	$\dot{m}_{22} = \dot{m}_{23} = \dot{m}_{R600a}$	$\dot{W}_{turb4.} = \dot{m}_{R600a}(h_{22} - h_{23})$	$\dot{S}_{gen,turb4.} = \dot{m}_{CO2}(s_{22} - s_{23})$	$\dot{E}x_{D,turb4.} = \dot{m}_{CO2}(ex_{22} - ex_{23}) - \dot{W}_{turb3.}$	$\psi_{turb4.} = \frac{\dot{W}_{turb3.}}{\dot{m}_{CO2}(ex_{22} - ex_{23})}$
R600a-heat exchanger VI (23-25)	$\dot{m}_{23} = \dot{m}_{25} = \dot{m}_{R600a}$	$\dot{Q}_{HX6}^{out} = \dot{m}_{R600a}(h_{23} - h_{25})$ $\dot{Q}_{HX6}^{in} = \dot{m}_{R600a}(h_{23} - h_{25}) * 1{,}4$	$\dot{S}_{gen.,HX6} = \dot{m}_{R600a}(s_{23} - s_{25}) + \left(\frac{\dot{Q}_{CO2}^{in}}{T_{HX6} - 2}\right)$	$\dot{E}x_{D,HX6} = \dot{m}_{R600a}(ex_{23} - ex_{25}) - \dot{Q}_{CO2}^{in}\left(1 - \frac{T_0}{T_{HX6} - 2}\right)$	$\psi_{HX5} = \frac{\dot{m}_{R600a}(ex_{23} - ex_{25})}{\dot{Q}_{CO2}^{in}\left(1 - \frac{T_0}{T_{HX6} - 2}\right)}$
R600a-pump (25-26)	$\dot{m}_{25} = \dot{m}_{26} = \dot{m}_{R600a}$	$\dot{W}_{pump} = \dot{m}_{R600a}(h_{26} - h_{25})$	$\dot{S}_{gen,pump} = \dot{m}_{R600a}(s_{26} - s_{25})$	$\dot{E}x_{D,pump} = \dot{m}_{R600a}(ex_{25} - ex_{26}) + \dot{W}_{pump}$	$\psi_{pump} = \frac{\dot{m}_{R600a}(ex_{26} - ex_{25})}{\dot{W}_{pump}}$

3. RESULTS

In Figure 3, the T-s diagram of the ideal brayton cycle for single stage (with regeneration) and double stage (with regeneration, intercooling and reheating) is given.

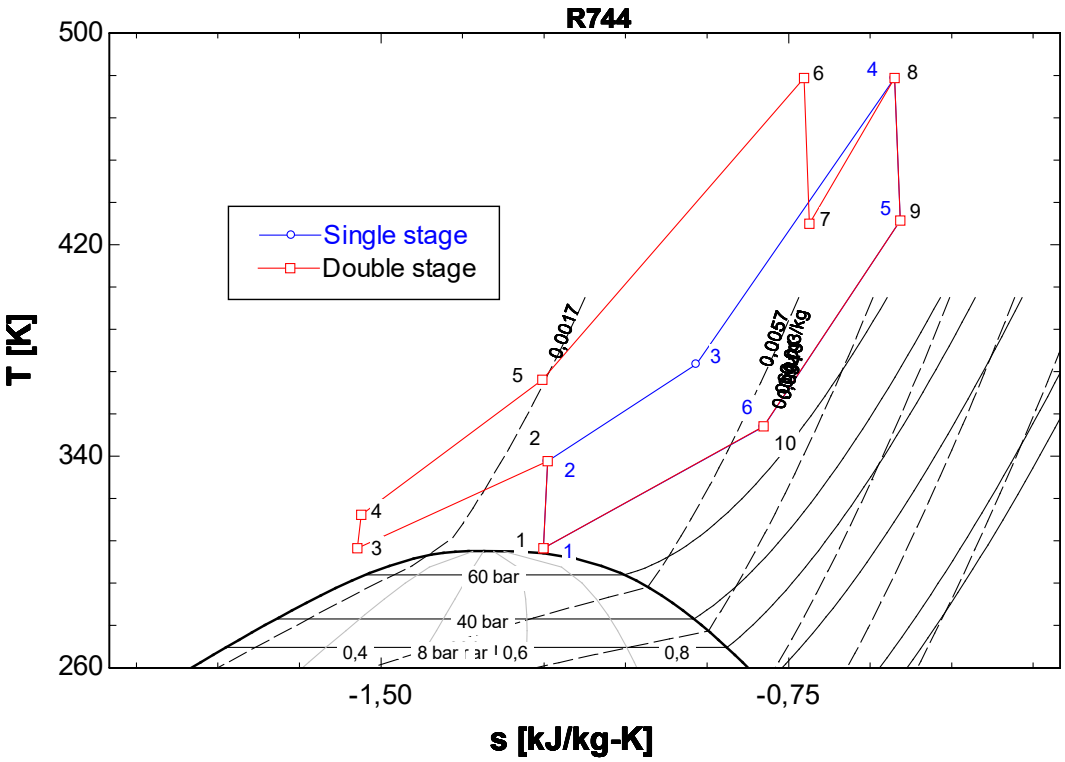

Figure 3. Single-stage and double-stage T-s cycle in the ideal brayton cycle

The cooling process at the 10th to 1st point of the T-s diagram in Figure 3 corresponds to the heat transfer between the 26th and 20th points in the system operating with the R600 refrigerant used in the ORC system in Figure 4.

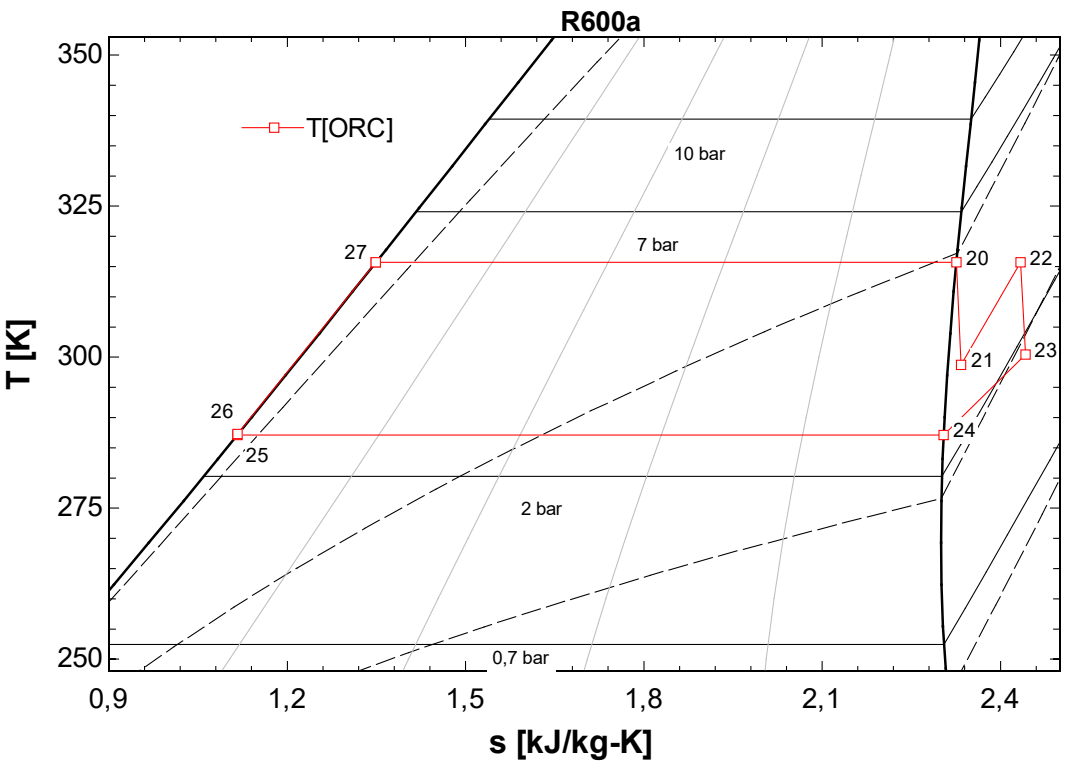

Figure 4. ORC system with R600a refrigerant

In Table 2, the thermodynamic values of the single-stage (regeneration) system are given according to the operating temperature data. (T_0(Dead state))

Table 2. Thermodynamic values of a single-stage (regeneration) system

Single stage	Temperature T [K]	Specific entropy s [kJ/kg.K]	Pressure P [bar]	Specific entalpy h [kJ/kg]	Exergy destruction Ex [kJ/kg]	Mass m [kg/s]
1	305.2	-1.201	75	-142.5	632.1	3
2	338.1	-1.194	135	-126	675.3	3
3	375.2	-0.9179	135	-28.3	725.7	3
4	483	-0.5551	135	125.3	867.3	3
5	429.2	-0.5445	75	84.6	735.9	3
6	351.2	-0.7966	75	-13.09	664.5	3
T_0	293.2	-0.01389	1	-5.125		

The thermodynamic results presented in Table 2 and the exergy destruction, exergy efficiencies and energy exchanges of each component of the system for the ideal single-stage (regeneration) Brayton cycle are shown in Table 3.

Table 3. Thermodynamic results of the one-stage (regenerated) ideal brayton cycle

Component	Exergy destruction Ex(KW)	Heat in Q(KW)in	Heat out Q(KW)out	Power W(KW)	Efficiency φ
1-2 compressors	6.454	-	-	49.57	0.87
2-3 Recuperators	20.94	293.1	293.1	-	0.70
3-4 Heat exchanger 1	66.95	645.1	460.8	-	0.68
4-5 Turbine1	9.311	-	-	122.1	0.93
5-6 Heat exchanger 2	47.29	277.3	388.3	-	0.46

As seen in Table 3, exergy destruction in the single-stage (with regeneration) system is seen in heat exchanger 1 with a maximum of 66.95KW. The best exergy efficiency was seen in turbine 1 with 93%. With a power of 72.53kw, it provided an electricity production efficiency of 40%. The thermodynamic data of the temperature results in the ideal brayton cycle in two stages (with regeneration, intercooling and reheating) are presented in Table 4.

Table 4. Thematic values of the double stage (regeneration, intercooling and reheating) cycle.

Double stage	Temperature T [K]	Specific entropy s [kJ/kg.K]	Pressure P [bar]	Specific entalpy h [kJ/kg]	Exergy destruction Ex [kJ/kg]	Mass m [kg/s]
1	305.2	-1.201	75	-142.5	632.1	3
2	338.1	-1.194	135	-136	675.3	3
3	305.2	-1.544	135	-239	644.4	3
4	317.8	-1.537	243	-223.8	683.4	3
5	361.6	-1.249	243	-126.1	723.6	3
6	483	-0.7217	243	92.28	914.7	3
7	427.9	-0.7118	135	54.08	791.4	3
8	483	-0.5444	135	125.3	867.3	3
9	429.2	-0.7965	75	84.63	735.9	3
10	351.2	-1.201	75	-13.05	664.5	3
T_0	293.2	-0.01389	1	-5.125		

The thermodynamic values of the cycle temperatures of the R600a refrigerant ORC system are presented in Table 5.

Table 5. Thermodynamic values of the cycle temperatures of the R600a refrigerant ORC system

ORC	Temperature T [K]	Specific entropy s [kJ/kg.K]	Pressure P [bar]	Specific entalpy h [kJ/kg]	Exergy destruction Ex [kJ/kg]	Mass m [kg/s]
20	315.7	2.326	5.668	611.7	65.09	0.951
21	298.7	2.333	3.149	591.1	43.38	0.951
22	315.7	2.434	3.149	621.9	44.70	0.951
23	300.4	2.442	1.749	600	21.61	0.951
25	287.1	1.116	2.503	232.7	41.89	0.951
26	287.3	1.116	5.668	233.4	42.42	0.951
T_0	293.2	2.487	1	590.6		

The thermodynamic calculation results of the cycles resulting in the combination of the two-stage (regeneration. intercooling and reheating) cycle and the ORC system are presented in Table 6.

Table 6. Thermodynamic results of the combination of the double stage (regeneration, intercooling and reheating) cycle with the ORC system.

Component	Exergy destruction Ex(KW)	Heat in Q(KW)in	Heat out Q(KW)out	Power W(KW)	Efficiency φ
1-2 compressors1	6.454	-	-	49.57	0.87
2-3 Heat exchanger 1	13.29	242.1	338.9	-	0.48
3.4 compressor2	6.305	-	-	45.49	0.86
4-5 Recuperators	31.28	293	293	-	0.56
5-6 Heat exchanger 2	91.84	917.3	655.2	-	0.67
6-7 Turbine1	8.756	-	-	114.6	0.93
7-8 Heat exchanger 3	32.5	299.2	213.7	-	0.68
8-9 Turbine2	9.311	-	-	122.1	0.93
10-1 Heat exchanger 4	9.72	359.8	388.4	-	0.70
20-21 Turbine 3	2.14	-	-	19.58	0.90
21-22 Heat exchanger 5	0.78	40.99	29.28	-	0.62

22-23 Turbine 4	2.26	-	-	20.83	0.90
23-25 Heat exchanger 6	3.87	249.5	349.3	-	0.80
25-26 Pump	0.09	-	-	0.628	0.84

In the ORC system, which is added by making use of waste heat in the regeneration, intercooling and reheating system, heat exchanger 1, which is used as the main heat source, followed by the recuperator, heat exchanger 1, heat exchanger 4, the heat exchangers have been subjected to exergy destruction. In terms of exergy efficiency, Turbine1, Turbine 2, Turbine 3, Turbine 4, respectively, were used with the highest efficiency.

The net work output and thermal efficiencies with the addition of the ORC system in the single and double-stage operating cycle are given in Table 7.

Table 7. Thermal efficiency of single and double stage cycle

Cycle	Heat input $\dot{Q}$(kW)	Heat output $\dot{Q}$(kW)	Net power $\dot{W}$(kW)	Energy efficiency ηth,
Single stage	$(h_4 - h_3) * \dot{m}_{co2}$	$(h_6 - h_1) * \dot{m}_{co2}$	72.57	0.157
Double stage	$[(h_6 - h_5) + (h_8 - h_7)] * \dot{m}_{co2}$	$[(h_{10} - h_1) + (h_2 - h_3)] * \dot{m}_{co2}$	171.45	0.197
ORC	$[(h_{20} - h_{26}) + (h_{22} - h_{21})] * \dot{m}_{R600a}$	$(h_{23} - h_{25}) * \dot{m}_{R600a}$	39.75	0.102

As can be seen in Table 7, when switching from single-stage to double-stage, there was an increase in electricity production of 136% and an increase in thermal efficiency of 22%. Adding ORC system to single-stage and double-stage system will increase thermal efficiency by 10,2% and net work by 39,75KW.

The exergy destruction and exergy efficiencies for each system are given in Table 8 with the addition of the ORC system in the single and double stage operating cycle.

Table 8. Exergy destruction and yields of single and double stage cycles

Cycle	Exergy in Ex(kW)	Exergy out Ex(kW)	Exergy desruction Ex(kW)	Exergy efficiency $\boldsymbol{\varphi_{Ex}}$
Single stage	$(ex_4 - ex_3) * \dot{m}_{co2}$	$(ex_6 - ex_1) * \dot{m}_{co2}$	109,2	0,77
Double stage	$[(ex_6 - ex_5) + (ex_8 - ex_7)] * \dot{m}_{co2}$	$[(ex_{10} - ex_1) + (ex_2 - ex_3)] * \dot{m}_{co2}$	203.7	0.76
ORC	$[(ex_{20} - ex_{26}) + (ex_{22} - ex_{21})] * \dot{m}_{R600a}$	$(ex_{23} - ex_{25}) * \dot{m}_{R600a}$	44.27	0.15

Table 8 When switching from single stage to double stage, exergy destruction increased by 86% and exergy efficiency decreased by 1%. Adding ORC system to single-stage and double-stage system will increase exergy efficiency by 15% and exergy destruction by 44.27KW.

4. CONCLUSIONS

Increasing and changing energy demand reminds us of the sustainable and most efficient use of energy day by day. In this context, it is inevitable that regenerative systems will provide us with more usable results. This study provides us with the final system improvements of CO_2 in supercritical Brayton cycles with intermediate heat exchangers, gradual compression, and gradual expansion. The performance characteristics of the CO_2 power systems and the

combined ORC system, and the energy and energy analysis results of the system components, by transferring the system from the waste heat source to the ORC cycle:

In the single-stage (with regeneration) system, exergy destruction is observed in heat exchanger 1 with a maximum of 66.95KW. The best energy efficiency was seen in turbine 1, with 93%. With a power of 72.53 kw, it provided an electricity production efficiency of 40%.

In the ORC system, which is added by making use of waste heat in the regeneration, intercooling, and reheating systems, heat exchanger 1 is used as the main heat source, followed by the recuperator, heat ext. 1, temp. At 4, the heat exchangers are subject to energy destruction. In terms of energy efficiency, turbine 1, turbine 2, turbine 3, and turbine 4, respectively, were used with the highest efficiency.

When switching from single-stage to double-stage, electricity production increased by 136% and thermal efficiency increased by 22%.Adding an ORC system to single-stage and double-stage systems will increase thermal efficiency by 10.2% and net work by 39.75KW.

When switching from single stage to double stage, increased by 86% and energy efficiency decreased by 1%. Adding an ORC system to single-stage and double-stage systems will increase energy efficiency by 15% and exergy destruction by 44.27KW.

More sustainable and environmentally friendly system designs can be developed by integrating ORC systems into recompression and reexpansion systems. The results obtained in this study show us that waste heat sources are of great importance in increasing the efficiency of integrated systems by combining energy conversion power plants and providing us with a more sustainable energy source.

REFERENCES

[1] Wang, E., Peng, N., & Zhang, M. (2021). System design and application of supercritical and transcritical CO_2 power cycles: A review. Frontiers in Energy Research, 699.

[2] Mishra, R. S., & Kumar, M. (2019). Thermodynamic analysis of brayton cycle for power generation.

[3] Bellos, E., & Tzivanidis, C. (2021). Parametric Analysis of a Polygeneration System with CO_2 Working Fluid. Applied Sciences, 11(7), 3215.

[4] Zhang, L., Deng, T., Klemeš, J. J., Zeng, M., Ma, T., & Wang, Q. (2021). Supercritical CO_2 Brayton cycle at different heat source temperatures and its analysis under leakage and disturbance conditions. Energy, 237, 121610.

[5] Zhang, R., Su, W., Lin, X., Zhou, N., & Zhao, L. (2020). Thermodynamic analysis and parametric optimization of a novel S–CO_2 power cycle for the waste heat recovery of internal combustion engines. Energy, 209, 118484.

[6] Hoang, H. T., Corcoran, M. R., & Wuthrich, J. W. (2009). Thermodynamic study of a supercritical CO_2 Brayton cycle concept. In Proceedings of supercritical CO_2 power cycle symposium.

[7] Wang, X., Wang, J., Zhao, P., & Dai, Y. (2016). Thermodynamic comparison and optimization of supercritical CO2 Brayton cycles with a bottoming transcritical CO_2 cycle. Journal of Energy Engineering, 142(3), 04015028.

[8] Yari, M., & Sirousazar, M. (2010). A novel recompression S-CO_2 Brayton cycle with pre-cooler exergy utilization. Proceedings of the Institution of Mechanical Engineers, Part A:

Journal of Power and Energy, 224(7), 931-946.

[9] Al-Sulaiman, F. A., & Atif, M. (2015). Performance comparison of different supercritical carbon dioxide Brayton cycles integrated with a solar power tower. Energy, 82, 61-71.

[10] Yu, W., Gong, Q., Gao, D., Wang, G., Su, H., & Li, X. (2020). Thermodynamic analysis of supercritical carbon dioxide cycle for internal combustion engine waste heat recovery. Processes, 8(2), 216.

[11] Ruiz-Casanova, E., Rubio-Maya, C., Pacheco-Ibarra, J. J., Ambriz-Díaz, V. M., Romero, C. E., & Wang, X. (2020). Thermodynamic analysis and optimization of supercritical carbon dioxide Brayton cycles for use with low-grade geothermal heat sources. Energy Conversion and Management, 216, 112978.

[12] Zhou, J., Zhang, C., Su, S., Wang, Y., Hu, S., Liu, L., ... & Xiang, J. (2018). Exergy analysis of a 1000 MW single reheat supercritical CO_2 Brayton cycle coal-fired power plant. Energy conversion and management, 173, 348-358.

[13] Chowdhury, J. I., Asfand, F., Hu, Y., Balta-Ozkan, N., Varga, L., & Patchigolla, K. (2019, January). Waste heat recovery potential from industrial bakery ovens using thermodynamic power cycles. In ECOS 2019-Proceedings of the 32nd International Conference on Efficiency, Cost, Optimization, Simulation and Environmental Impact of Energy Systems (pp. 2435-2441). Institute of Thermal Technology.

[14] Wang, K., Li, M. J., Guo, J. Q., Li, P., & Liu, Z. B. (2018). A systematic comparison of different S-CO_2 Brayton cycle layouts based on multi-objective optimization for applications in solar power tower plants. Applied energy, 212, 109-121.

[15] Gao, W., Yao, M., Chen, Y., Li, H., Zhang, Y., & Zhang, L. (2019). Performance of S-CO_2 Brayton cycle and organic Rankine cycle (ORC) combined system considering the diurnal distribution of solar radiation. Journal of Thermal Science, 28(3), 463-471.

[16] Ma, H., & Liu, Z. (2022). An Engine Exhaust Utilization System by Combining CO_2 Brayton Cycle and Transcritical Organic Rankine Cycle. Sustainability, 14(3), 1276.

[17] Li, B., Wang, S. S., Wang, K., & Song, L. (2021). Comparative investigation on the supercritical carbon dioxide power cycle for waste heat recovery of gas turbine. Energy Conversion and Management, 228, 113670.

[18] Purjam, M., Goudarzi, K., & Keshtgar, M. (2017). A new supercritical carbon dioxide brayton cycle with high efficiency. Heat Transfer—Asian Research, 46(5), 465-482.

[19] Padilla, R. V., Benito, R. G., & Stein, W. (2015). An exergy analysis of recompression supercritical CO_2 cycles with and without reheating. Energy Procedia, 69, 1181-1191.

[20] Besarati, S. M., & Yogi Goswami, D. (2014). Analysis of advanced supercritical carbon dioxide power cycles with a bottoming cycle for concentrating solar power applications. Journal of solar energy engineering, 136(1).

[21] Akbari, A. D., & Mahmoudi, S. M. (2014). Thermoeconomic analysis & optimization of the combined supercritical CO_2 (carbon dioxide) recompression Brayton/organic Rankine cycle. Energy, 78, 501-512.

[22] Khan, Y., & Mishra, R. S. (2021). Performance evaluation of solar based combined pre-compression supercritical CO_2 cycle and organic Rankine cycle. International journal of Green energy, 18(2), 172-186.

[23] Chacartegui, R., Sánchez, D., Muñoz, J. M., & Sánchez, T. (2009). Alternative ORC bottoming cycles for combined cycle power plants. Applied Energy, 86(10), 2162-2170.

[24] Dincer, I., & Rosen, M. A. (2012). Exergy: energy, environment and sustainable development. Newnes.

[25] Cengel, Y. A., Boles, M. A., & Kanoğlu, M. (2011). Thermodynamics: an engineering approach (Vol. 5, p. 445). New York: McGraw-hill.

[26] Klein, S. A., & Alvarado, F. L. (2002). Engineering equation solver. F-Chart Software, Madison, WI, 1.